Reproductive Sciences (2021) 28:1718–1732
https://doi.org/10.1007/s43032-021-00499-1

INFERTILITY: ORIGINAL ARTICLE

# Human Umbilical Cord Mesenchymal Stem Cells Improve Ovarian Function in Chemotherapy-Induced Premature Ovarian Failure Mice Through Inhibiting Apoptosis and Inflammation via a Paracrine Mechanism

Taoran Deng[1] · Jing He[2] · Qingyun Yao[1] · Linjing Wu[1] · Liru Xue[3] · Mingfu Wu[3] · Dongcheng Wu[2,4] · Changyong Li[5] · Yufeng Li[1]

Received: 6 July 2020 / Accepted: 14 February 2021 / Published online: 9 March 2021


## Abstract

Human umbilical cord mesenchymal stem cell (UC-MSC) application is a promising arising therapy for the treatment of premature ovarian failure (POF). However, little is known about the inflammation regulatory effects of human umbilical cord MSCs (UC-MSCs) on chemotherapy-induced ovarian damage, regardless of in vivo or in vitro. This study was designed to investigate the therapeutic effects of UC-MSC transplantation and underlying mechanisms regarding both apoptosis and inflammation in POF mice. The chemotherapy-induced POF models were induced by intraperitoneal injection of cyclophosphamide. Ovarian function parameters, granulosa cell (GC) apoptosis, and inflammation were examined. Morphological staining showed that UC-MSC treatment increased the ovary size, and the numbers of primary and secondary follicles, but decreased the number of atretic follicles. Estradiol levels in the UC-MSC-treated group were increased while follicle-stimulating hormone levels were reduced compared to those in the POF group. UC-MSCs inhibited cyclophosphamide-induced GC apoptosis and inflammation. Meanwhile, phosphorylation of AKT and P38 was elevated after UC-MSC treatment. Tracking of UC-MSCs in vivo indicated that transplanted UC-MSCs were only located in the interstitium of ovaries rather than in follicles. Importantly, UC-MSC-derived extracellular vesicles protected GCs from alkylating agent–induced apoptosis and inflammation in vitro. Our results suggest that UC-MSC transplantation can reduce ovary injury and improve ovarian function in chemotherapy-induced POF mice through anti-apoptotic and anti-inflammatory effects via a paracrine mechanism.

**Keywords** Umbilical cord mesenchymal stem cell · Premature ovarian failure · Inflammation · Apoptosis · Extracellular vesicle

## Introduction

Premature ovarian failure (POF) is characterized by amenorrhea or oligomenorrhea and high level of follicle-stimulating hormone (FSH) in females under the age of 40 years. POF is the loss of ovarian function, resulting in clinical manifestations including the early occurrence of menopausal syndromes and infertility. As a common disease in the fields of gynecological endocrine and reproductive medicine, the prevalence of POF is around 1% [1]. Chemotherapy is a common cause for POF, depending on the drug and dose. Some chemotherapy regimens are considered more gonadotoxic, and alkylating agents (e.g., cyclophosphamide) have been strongly evidenced as highly ovotoxic [2]. Previous studies reported that ovarian failure was caused in 42–80% of women treated with alkylating agents [3–5]. Hormone replacement therapy (HRT) is the first-line therapy for POF, aiming to treat

✉ Changyong Li
lichangyong@whu.edu.cn

✉ Yufeng Li
tjlyf66@126.com

[1] Reproductive Medicine Center, Tongji Hospital, Tongji Medical College, Huazhong University of Science and Technology, Wuhan 430030, Hubei, China

[2] Department of Biochemistry and Molecular Biology, School of Basic Medical Sciences, Wuhan University, Wuhan 430072, Hubei, China

[3] Department of Obstetrics and Gyneacology, Tongji Hospital, Tongji Medical College, Huazhong University of Science and Technology, Wuhan 430030, Hubei, China

[4] Wuhan Hamilton Biotechnology-Co., LTD, Wuhan 430075, Hubei, China

[5] Department of Physiology, School of Basic Medical Sciences, Wuhan University, Wuhan 430072, Hubei, China

vasomotor and genito-urinary symptoms, maintain bone health, and prevent osteoporosis and cardiovascular disease, whereas HRT could not effectively restore the impaired ovarian function [6]. In recent years, there were promising advances in mesenchymal stem cells (MSCs) for treating POF, drawing attention to their clinical application value for improving ovarian function.

MSCs are characterized by self-renewal property, high proliferation rate, and multipotent differentiation capacity. They have been used to treat numerous severe and resistant diseases, including lung injury, nephropathy, osteoarthritis, nervous system diseases, intrauterine adhesion, and POF [7–12]. MSCs promote the damaged tissue repair and regeneration predominantly via differentiation into the target tissue cells, anti-apoptosis effects, and strong capacities of immune regulation and inflammation inhibition. Human umbilical cord MSCs (UC-MSCs) are distinguished due to their "younger" somatic stem cell nature, extremely poor immunogenicity, low tumorigenicity, rapid proliferation speed, and fewer ethical issues [13]. Therefore, UC-MSCs have recently become a promising candidate for clinical applications. Although UC-MSCs have currently been used to treat POF in some clinical trials, the mechanisms underlying their restorative effects are not fully understood.

The anti-apoptotic effect is one of the critical mechanisms of UC-MSCs to protect ovarian granulosa cells (GCs). There has been evidence showing that rapidly proliferative cells (GCs) are more sensitive to the cytotoxicity of alkylating agents than the cells at rest (oocytes), implying steroidogenic cells in the follicle are more likely the target of cyclophosphamide (CTX) [14]. Previous studies showed that chemotherapeutic drugs induced apoptosis of GCs, and MSC transplantation could downregulate the apoptotic levels of GCs [15–18]. Hence, the alleviation degree of GC apoptosis is an important parameter to evaluate the restorative effects of UC-MSCs for treating POF.

CTX has been reported to cause inflammatory imbalance in the ovaries [19, 20]. On the other hand, anti-inflammation and immune regulation capacities of MSCs were proven to be critical for treating inflammatory lesions and immune disorders, such as osteoarthritis and systematic lupus erythematosus [9, 21]. Although a few studies reported that MSCs from other sources could reduce the production of pro-inflammatory cytokines in damaged ovaries [19, 22, 23], little is known about the inflammation regulatory effects of UC-MSCs on chemotherapy-induced ovarian damage.

Intravenously injected MSCs have been evidenced to be able to migrate to the ovary tissue in the POF model [22, 24–26]. MSCs derived from various sources other than endometrium [26] were shown to locate in the stroma of the ovaries, but not differentiate into follicular cells. Additionally, MSC-derived materials also revealed protective effects for the ovaries against chemotherapy [27–30]. Those results strongly suggested the potential role of a paracrine mechanism. In recent years, extracellular vesicles (EVs), a class of membranous nanoparticles secreted by mammalian cells, have been found to serve as cell-cell communication vehicles and participate in the paracrine effects [31]. The application of MSC-EV-related studies would further evidence the significance of a paracrine mechanism and help reveal the mechanisms underlying the effectiveness of MSCs in vitro.

In the current study, we aimed to investigate the mechanisms with respect to apoptosis and inflammation underlying the therapeutic effects of UC-MSCs on chemotherapy-induced ovary damage, both in vivo and in vitro. Moreover, UC-MSC-derived EVs were used to explore the role of a paracrine mechanism underlying the reparative effects of UC-MSCs.

## Materials and Methods

### Animals

The female C57BL/6 mice (6–7 weeks old) were purchased from Hubei Provincial Center for Disease Control and Prevention. They were bred at a temperature of 30 ± 2 °C with a 12-h light/dark cycle.

### Cells

**Isolation and Identification of UC-MSCs** UC-MSCs were obtained from Hamilton Biotech Co., Ltd., Hubei province. The preparation was as follows: the full-term umbilical cord (UC) was retrieved from a healthy newborn after obtaining the informed consent of its mother. UC was dissected into 1.5–2.0-cm sections, and Wharton's Jelly was isolated from UC. The homogenates of Wharton's Jelly were washed and plated in a cell culture dish containing BioWhittaker ultraCULTURE general purpose serum-free medium (Lonza, Basel, Switzerland) supplemented with 10% Ultroser G serum substitute (Pall, Port Washington, NY, USA) and glutamine (Lonza) at 37 °C, 5% $CO_2$. After 13 days, nonadherent cells were removed, and the remaining cells were identified as the primary passage of UC-MSCs. Passage 5 (P5) UC-MSCs were applied for the following experiments.

The morphology of UC-MSCs was observed using a light microscopy. Flow cytometry was used to identify the phenotype of UC-MSCs. Positive markers CD105, CD73, CD90, and CD44 as well as negative markers CD19, CD34, and HLA-DR (all from BioLegend, San Diego, USA) were used for MSC biomarker detection. For in vitro differentiation assays, UC-MSCs were plated with a density of $1 \times 10^3$ cells/$cm^2$ in 24-well plates. To achieve adipogenic differentiation, UC-MSCs were cultured in adipogenic differentiation medium (Weitong, Shenzhen, China) for 14 days. They were fixed

with 4% paraformaldehyde and stained with Oil Red O. To achieve osteogenic differentiation, UC-MSCs were cultured in osteogenic differentiation medium for 21 days. Cells were fixed, and mineral deposition was visualized using 0.1% Alizarin Red.

**Culture of KGN Cells** KGN cells were purchased from the Cell Bank of Wuhan University. They were cultured in DMEM (Gibco by Thermo Fisher Scientific, NY, USA) containing 10% fetal bovine serum (Gibco by Life Technologies, NY, USA) at 37 °C, 5% $CO_2$.

## Isolation and Characterization of EVs from UC-MSCs

The conditioned medium of UC-MSCs was collected after 72 h. The medium was processed by 300*g* centrifugation for 10 min and 2000*g* centrifugation for 20 min to remove cell debris. Ultrafiltration of UC-MSCs was conducted using 100 kDa AmiconUltra-4 (Millipore, Darmstadt, Germany) by 5000*g* centrifugation for 30 min. The concentrated medium was ultracentrifuged at 100,000*g* for 70 min at 4 °C. The supernatant was removed, and pellets were resuspended in PBS. The solution was subsequently ultracentrifuged at 100,000*g* for 70 min at 4 °C. The EV pellets were resuspended in PBS and stored at −80 °C for further use.

The morphology of EVs was observed using TEM. Positive biomarkers Alix and CD9 (Affinity Biosciences, OH, USA) as well as negative biomarker Calnexin (Cell Signaling Technology, MA, USA) were used for western blotting to identify EVs. To examine the size distribution of EVs, nanoparticle tracking analysis was conducted by ZetaView PMX 110 (Particle Metrix, Germany).

## Induction of POF Model and UC-MSC Treatment

Mice were randomly divided into four groups: normal control (NC) group, NC + UC-MSC group, POF group, and UC-MSC treatment group. The POF group mice ($n$ = 8) were intraperitoneally injected with 120 mg/kg of cyclophosphamide (CTX, Sigma-Aldrich, USA) and 30 mg/kg busulfan. For the NC group ($n$ = 6) and NC + UC-MSC group ($n$ = 5), 400 μL PBS instead of chemotherapeutic drugs was intraperitoneally injected into mice. Seven days after POF induction, POF mice in the UC-MSC treatment group ($n$ = 8) were intravenously injected with $1 \times 10^6$ UC-MSCs in 200 μL PBS and received a second injection after 2 days. Mice in the POF group and NC + UC-MSC group received 200 μL PBS twice to serve as control.

To induce the chemotherapy-induced POF cell model, KGN cells were cultured with 5 μg/mL nitrogen mustard (NM) (mechlorethamine hydrochloride, Macklin, Shanghai, China), an activated metabolite of CTX, for 48 h. To investigate whether UC-MSCs protect the ovarian functions via a paracrine pathway, KGN cells were co-cultured with 5 μg/mL NM and 150 μg/mL UC-MSC-EVs for 48 h.

## Ovarian Function Assessment

Estrus cycle determination, counting of follicles in different stages, and enzyme-linked immunosorbent assay (ELISA) for FSH and E2 were performed as detailed in the supplemental materials.

## Gene and Protein Expression Measurement

Real-time quantitative PCR, ELISA, immunohistochemistry, and western blot analysis were performed as described in supplemental methods.

## Tracking of UC-MSCs In Vivo

To determine the location of the injected UC-MSCs in the ovaries, three cell tracking methods were performed. Seven days after POF model induction, a total of $1 \times 10^6$ BrdU-labeled (BioLegend) or GFP-labeled UC-MSCs in 200 μL PBS was tail intravenously injected into the mice and injected a second time on the third day. Two weeks after the UC-MSC treatment, the ovaries were extracted and immediately frozen by liquid nitrogen. The frozen sections of ovarian samples were used to investigate the location of UC-MSCs under a fluorescence microscope. Nuclei were stained by DAPI. Meanwhile, paraffin sections of the ovaries were applied for UC-MSCs tracking by performing immunohistochemistry using mouse anti-human nuclei monoclonal antibody (Millipore).

## Transwell Migration Assay

To examine the migration capacity of UC-MSCs towards the lesions, transwell assays were used with ovary extracts. In order to prepare ovary extracts, the ovary tissues were removed at 7 days after treating with or without CTX and subsequently homogenized by adding the culture medium free of serum substitute (150 mg tissue/mL culture medium). After being starved for 24 h, UC-MSCs were seeded with a density of $5 \times 10^5$ cells in 200 ul culture medium without serum substitute in the upper Transwell chamber (#3422, Corning, NY, USA). The lower chambers were filled with 500 μL culture medium without serum substitute but containing 20% ovary extract supernatant. Following 24-h incubation, cells on the upper side of the membrane were removed using cotton swabs, while cells on the bottom side of the membrane were stained with 0.1% crystal violet and counted in five randomly selected microscopic fields (×400).

### Survival and Apoptosis Detection

CCK-8 assay and annexinV and propidium iodide (PI) staining were conducted according to the details in the supplemental data.

### Statistical Analysis

Data were expressed as mean ± SD. All analyses were performed using GraphPad Prism 8 (GraphPad Software Inc., CA, USA). One-way analysis of variance (ANOVA) and independent-samples *t* test were respectively used for multiple- and two-group comparisons. If there was a significant difference of variance, then the Mann-Whitney test was performed for two-group comparisons. $P < 0.05$ was considered statistically significant.

## Results

### Identification and Characterization of UC-MSCs

P5 UC-MSCs were used in this study, and they were identified according to morphology, differentiation capacities, and MSC surface markers. UC-MSCs showed a fibroblast-like spindle morphology (Fig. 1a). To determine whether UC-MSCs could be induced and differentiated into adipocytes and osteoblasts, cells were respectively stained with Oil Red O and Alizarin Red. Figure 1 b and c demonstrated the adipogenic and osteogenic differentiation capacities of UC-MSCs. Additionally, flow cytometry was used to detect the expression of MSC surface markers of P5 UC-MSCs. As shown in Fig. 1d, more than 98% of UC-MSCs were positive for the markers CD44, CD105, CD73, CD90, and CD44. Meanwhile, UC-MSCs were negative for markers CD19, CD34, and HLA-DR (positive proportion < 1%).

UC-MSC Treatment Improved Ovarian Function in POF mice

To evaluate the effects of UC-MSC treatment on ovarian function in POF mice, we recorded 3 weeks of body weight changes and estrus cycles at 7 days after treatments, and other ovarian function parameters among the three groups at 2 and 4 weeks after treatments (Fig. 2a). In the POF group, the body weight increased slowly especially during the first week after saline treatments. However, the body weight of POF mice treated with UC-MSCs increased fast during 2 weeks after the treatments compared to that of mice in the POF group. To be noted, there was a slight decrease in body weight of the UC-MSC group after 19 days following the treatments (Fig. 2b).

We also assessed the estrus cycles in the three groups. POF mice had longer duration of estrus cycles compared to the normal control (NC) group (5.21 ± 0.76 vs 4.14 ± 0.35 days, $P < 0.01$), whereas UC-MSC treatment could reduce the duration (4.25 ± 0.29 vs. 5.21 ± 0.76 days, $P = 0.02$). Besides, chemotherapy induced a significantly higher diestrus percentage (52.29% ± 15.25% vs. 29.27% ± 7.67%, $P < 0.01$), while UC-MSC treatment reversed the diestrus percentage to a normal level (32.86% ± 9.13% vs. 52.29% ± 15.25%, $P < 0.01$; Fig. 2c).

The serum hormone levels were examined in the three groups at 2 and 4 weeks after the treatments. At 2 weeks following the treatments, the level of FSH was significantly lower, while the level of E2 was higher in the UC-MSC group compared to that in the POF group (6.49 ± 2.88 vs. 16.87 ± 2.96 mIU/mL, $P < 0.01$; 114.5 ± 21.38 vs. 70.29 ± 33.17 ng/mL, $P = 0.02$). At 4 weeks, the differences in hormone levels between the POF group and UC-MSC group turned to be smaller and nonsignificant (9.87 ± 8.35 vs. 16.45 ± 9.21 mIU/mL, $P = 0.16$; 89.61 ± 62.51 vs. 76.16 ± 34.05 ng/mL, $P = 0.61$; Fig. 2d).

The ovaries in the three groups were collected for pathological analysis. After 2 and 4 weeks, the ovaries in the POF group were more atrophic than those in the NC group, whereas UC-MSC treatment reverses the ovary size to some degree (Fig. 2e). Likewise, the ovarian follicles in the UC-MSC group were more than those in the POF group (Fig. 2f). Furthermore, we quantified the numbers of follicles at different stages among the three groups. After 2 weeks, there were significantly more primary follicles and secondary follicles as well as fewer atretic follicles in the UC-MSC group compared to those in the POF group (4.93 ± 2.12 vs. 1.86 ± 0.82 per slide, $P = 0.004$; 2.68 ± 1.44 vs. 1.35 ± 0.92 per slide, $P = 0.045$; 1.78 ± 0.56 vs. 3.22 ± 1.66 per slide, $P = 0.047$). After 4 weeks, there were modest but insignificant increase in secondary follicle number (1.75 ± 0.85 vs. 1.13 ± 0.89 per slide, $P > 0.05$) and decrease of atretic follicle number (2.40 ± 0.77 vs. 2.91 ± 1.49 per slide, $P > 0.05$) in the UC-MSC group compared to those in the POF group, whereas the difference of primary follicle numbers (3.90 ± 1.24 vs. 1.68 ± 0.88 per slide, $P = 0.001$) remained significant (Fig. 2g).

After the slowly intravenous administration of UC-MSCs, all 10 mice in the NC + UC-MSC group stayed alive. There were no significant differences in the body weight change, estrus cycle duration, sexual hormone levels, or the counts of follicles in various stages between the NC group and the NC + UC-MSC group (Fig. S1). Hence, intravenously UC-MSC treatment was a safe approach and would not affect the ovarian function of mice. The NC + UC-MSC group was not included in the subsequent experiments.

### UC-MSCs Reduced Apoptosis of Granulosa Cells

GCs regulate the development of oocytes and follicles, and they have been proven as the target of cytotoxic drugs. According to the above results, the ovarian protective

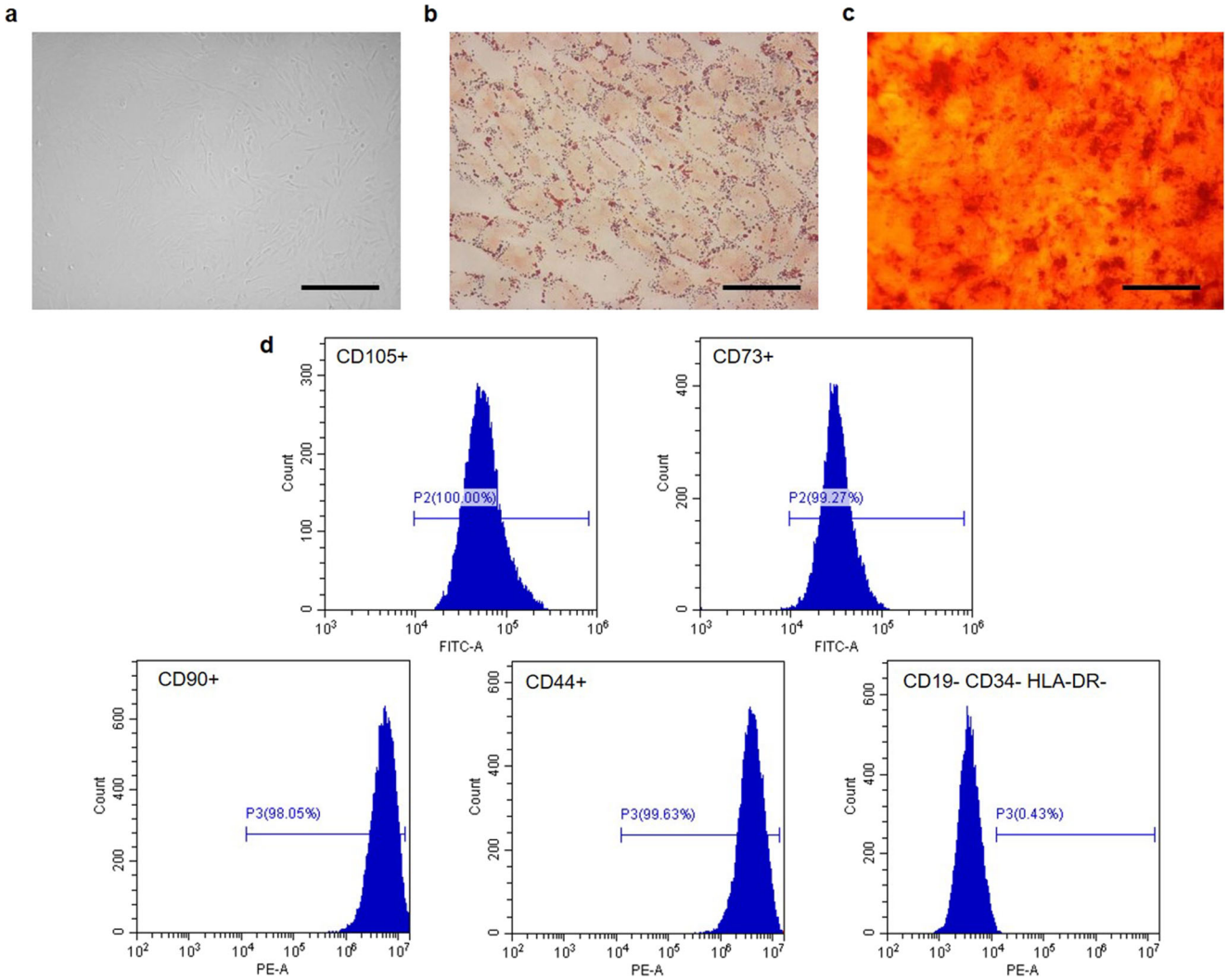


**Fig. 1** Identification of UC-MSCs. **a** Morphology of UC-MSCs. **b** Adipogenic differentiation of UC-MSCs. **c** Osteogenic differentiation of UC-MSCs. **d** Flow cytometric analysis of surface immune antigens of UC-MSCs. Scale bar = 50 μm

effects at 2 weeks after a single course of UC-MSC treatment were more significant than those shown at 4 weeks. Therefore, TUNEL staining and the detection of apoptosis-related protein expression after 2 weeks were conducted to explore the effectiveness of UC-MSCs against chemotherapy-induced GC apoptosis. In the follicle area, TUNEL-positive GCs could be clearly observed in the POF group. At 2 weeks after UC-MSC transplantation, TUNEL-positive GCs were dramatically decreased (Fig. 3a).

To further study the potential pathways involved in the regulation of GC apoptosis by UC-MSCs, the expression levels of apoptosis-related pathways in ovary tissues after 2 weeks were examined among the three groups. Cleaved caspase-3 was highly expressed in chemotherapy-induced injured ovaries, but its expression levels in the NC group and UC-MSC group were low, which was consistent with the TUNEL staining results. The expression ratio of pro-apoptosis protein Bax and anti-apoptosis protein Bcl-xl were significantly higher in the POF group compared to that in the UC-MSC group. As potential cell apoptosis and proliferation regulation proteins, the expression of AKT, p-AKT, P38, and p-P38 was also attempted in this study. UC-MSC treatment upregulated the phosphorylation level of AKT compared to that in the POF group, implying that the activation of the AKT pathway showed anti-apoptotic effects. On the other hand, phosphorylated P38/total P38 was higher compared to that in the POF group, indicating that its pro-proliferation effect took predominance (Fig. 3b).

## UC-MSCs Inhibited the Ovarian Inflammation in POF Mice

To determine the effect of UC-MSC transplantation on ovarian inflammation induced by chemotherapy, the levels

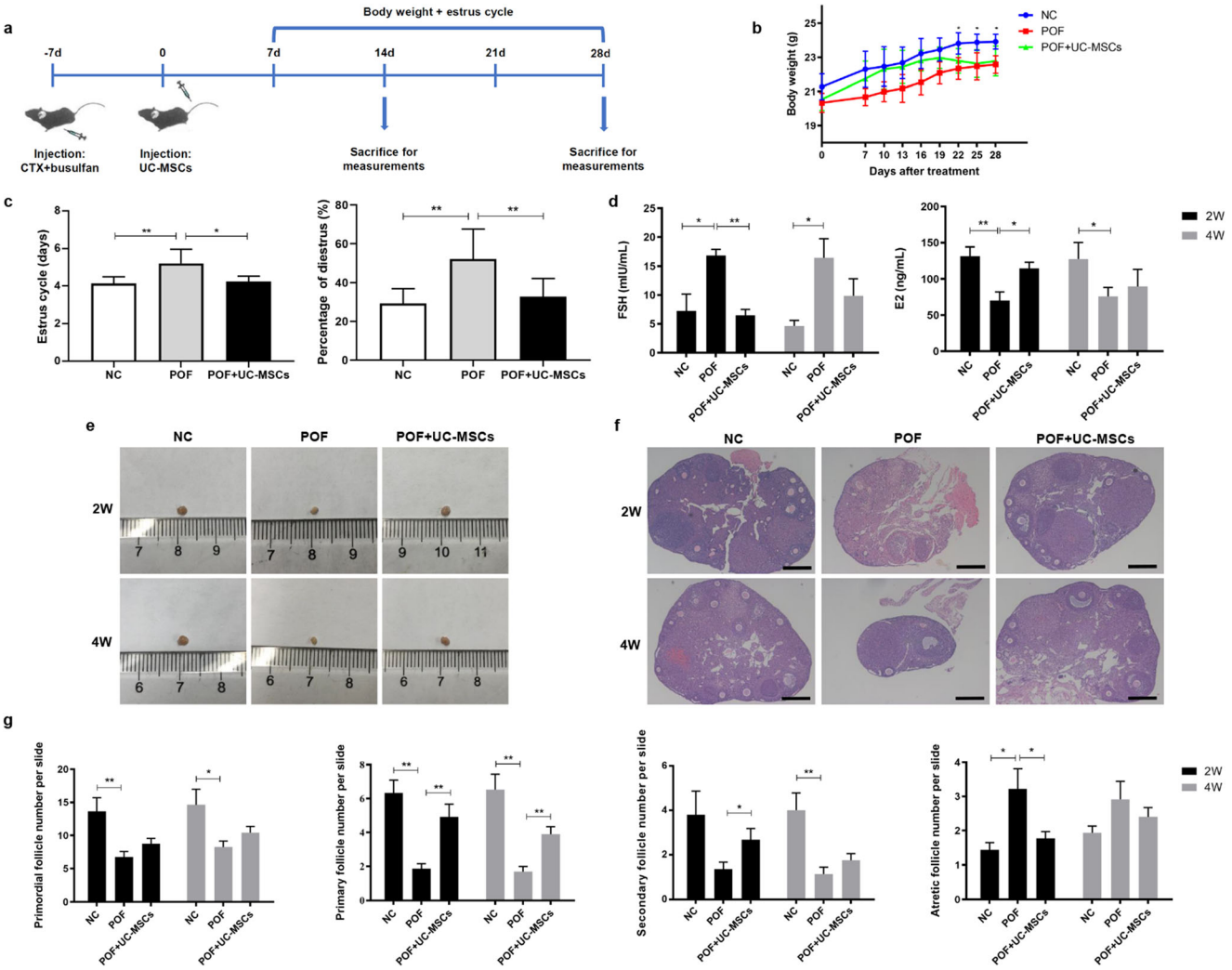


**Fig. 2** UC-MSC treatment improved ovarian function of POF mice. **a** Schematic of the experimental procedures for examining the therapeutic effects of UC-MSCs in POF mice. $N = 6–8$ mice/group. **b** The body weight changes during the 4 weeks after treatments. **c** Estrus cycle duration and percentage of diestrus during the 4 weeks after treatments. **d** The serum FSH and E2 concentrations after 2 and 4 weeks. **e** Macroscopic ovarian sizes after 2 and 4 weeks. **f** Representative images of H&E-stained ovary tissue sections after 2 and 4 weeks. **g** The quantities of primordial follicles, primary follicles, secondary follicles, and atretic follicles per slide in the three groups at 2 and 4 weeks after treatments. $^{*}P < 0.05$. $^{**}P < 0.01s$

of several inflammatory cytokines (pro-inflammatory cytokines: IL-6, IL-1β, TNF-α; anti-inflammatory cytokines: IL-10, IL-1RA, TSG-6) and VEGF of the ovary tissues were screened at 2 weeks after the treatments. Compared to those in the NC group, the mRNA levels of IL-6 were significantly increased while IL-10, TSG-6, and VEGF were decreased in the POF group. UC-MSC treatment significantly downregulated the mRNA expression of IL-6 and IL-1β, while it upregulated the mRNA expression of IL-10, TSG-6, and VEGF (Fig. 4a). The protein expression of pro-inflammatory cytokines in the ovary tissues was verified by ELISA and immunohistochemistry. Consistent with the mRNA results, UC-MSC transplantation significantly attenuated the levels of IL-6 and IL-1β, whereas it increased the VEGF level in POF mice (Fig. 4 b and c). MPO-positive cells demonstrated neutrophils. The neutrophil percentage in the POF group was higher than that in the NC group, while UC-MSC treatments significantly decreased the neutrophil percentage (Fig. 4c).

To further evaluate the inflammation condition in the ovaries, the infiltration of macrophages ($F4/80^{+}$ cells) and neutrophils ($Ly6G^{+}$ cells) was assessed. Chemotherapy induced abundant macrophage and neutrophil infiltration into the ovaries. Macrophages were extensively distributed in the ovaries, but predominantly located in the corpus luteal and atretic follicles. The majority of neutrophils were located surrounding and within the corpus luteal and follicles. However, UC-MSC transplantation attenuated the inflammatory cell infiltration (Fig. 4d). Negative controls of immunohistochemical experiments are shown in Fig. S2a.

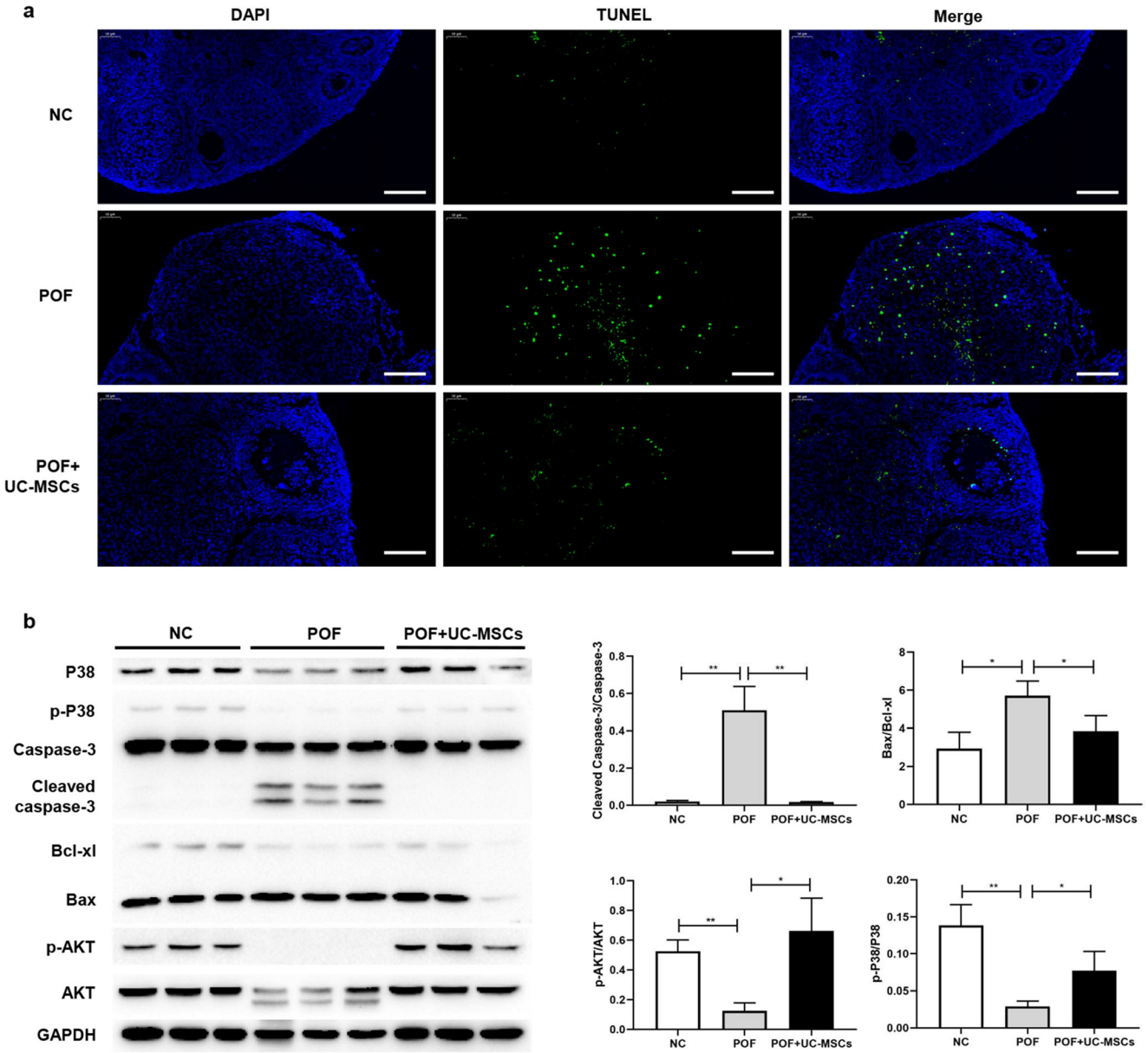


**Fig. 3** UC-MSCs attenuated the apoptotic level of injured ovaries. **a** Representative images of TUNEL staining to detect apoptosis of ovarian granulosa cells in vivo at 2 weeks after treatments. Scale bar = 100 μm. **b** Expressions of Bax, Bcl-xl, p-P38, P38, caspase-3, cleaved caspase-3, p-AKT, and AKT in the ovary tissues were detected by the western blot assay. GAPDH was used as the internal control. $*P < 0.05$. $**P < 0.01$

## Intravenously Injected UC-MSCs Were Located in the Interstitium of the Ovary Tissue

We traced the fate of tail intravenously administered UC-MSCs in POF mice using three different approaches (BrdU-UC-MSCs, GFP-UC-MSCs, and immunohistochemistry with anti-human nuclei monoclonal). As shown in Fig. 5 a, b, and c, UC-MSCs were located in the interstitial area but not in follicles of the ovary tissue. This result suggested that intravenous injected UC-MSCs could migrate into the ovary, but not differentiate into follicle component cells, indicating the significant role of a paracrine mechanism. Negative controls of immunohistochemical and immunofluorescent experiments are shown in Fig. S2.

Moreover, we investigated whether the chemotherapy-induced injured ovaries could serve as the chemotaxis source and lead UC-MSCs into the lesion. Nevertheless, the numbers of migrating UC-MSCs were similar with or without the stimulation of injured ovary extracts using the Transwell system (Fig. 5 d and e). A series of chemokines in the ovary tissues and their receptors on UC-MSCs were screened for mRNA expression differences between the NC group and POF group. However, we found no significant chemotaxis axis induced by ovarian injury (Fig. 5f).

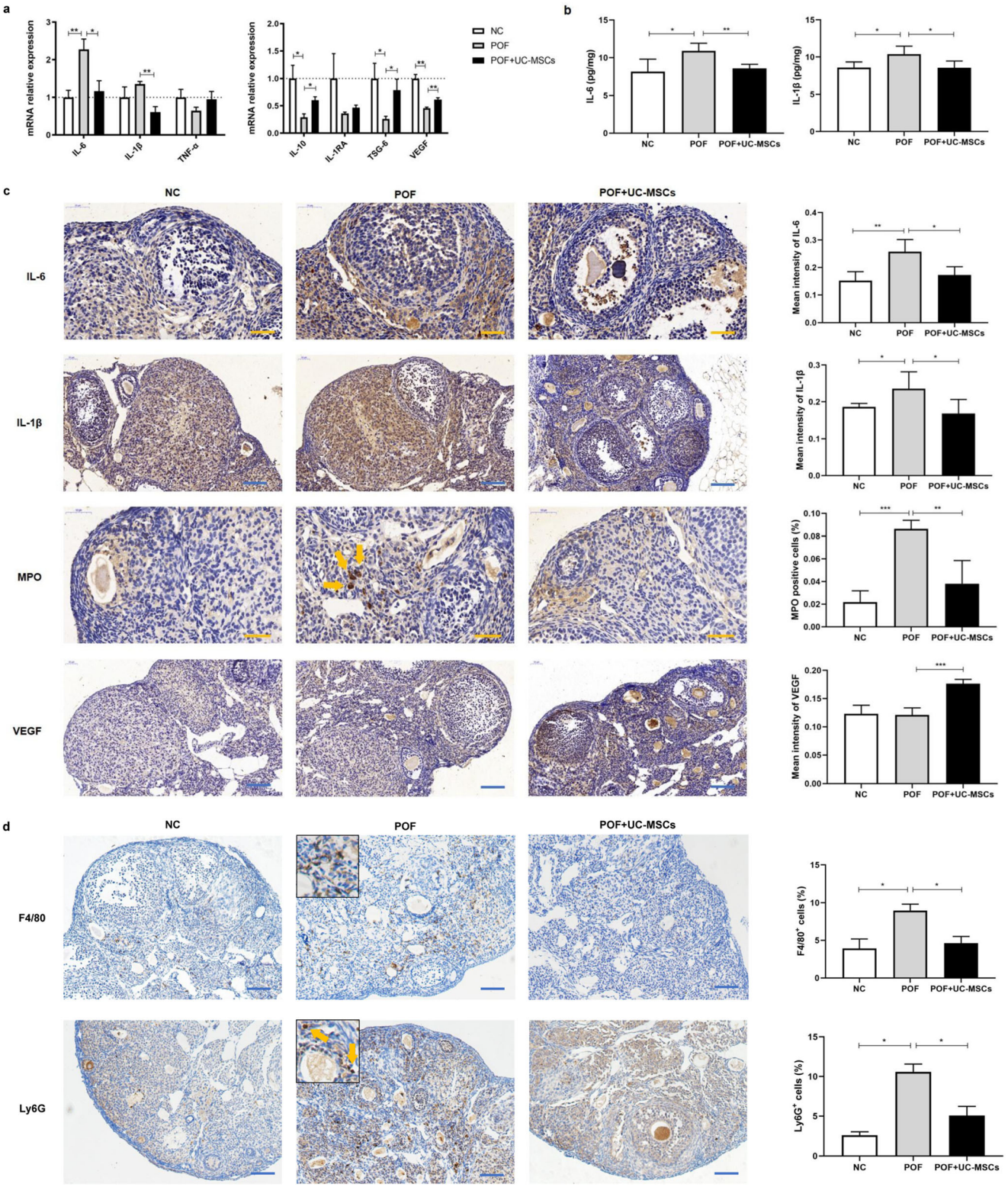


**Fig. 4** UC-MSCs inhibited the inflammation of injured ovaries at 2 weeks after treatments. **a** The mRNA levels of pro-inflammatory factors and anti-inflammatory factors. **b** The IL-6 and IL-1β concentrations of the ovary tissues (adjusted by the protein concentrations) in each group. **c** Representative images of immunohistochemistry and semi-quantitative comparisons among the three groups for IL-6, IL-1β, MPO, and VEGF. **d** Representative images of immunohistochemistry and semi-quantitative comparisons among the three groups for F4/80$^+$ and Ly6G$^+$ cells. Yellow scale bar = 50μm. Blue scale bar = 100 μm. The yellow arrow represents the typical stained neutrophil. *$P < 0.05$. **$P < 0.01$

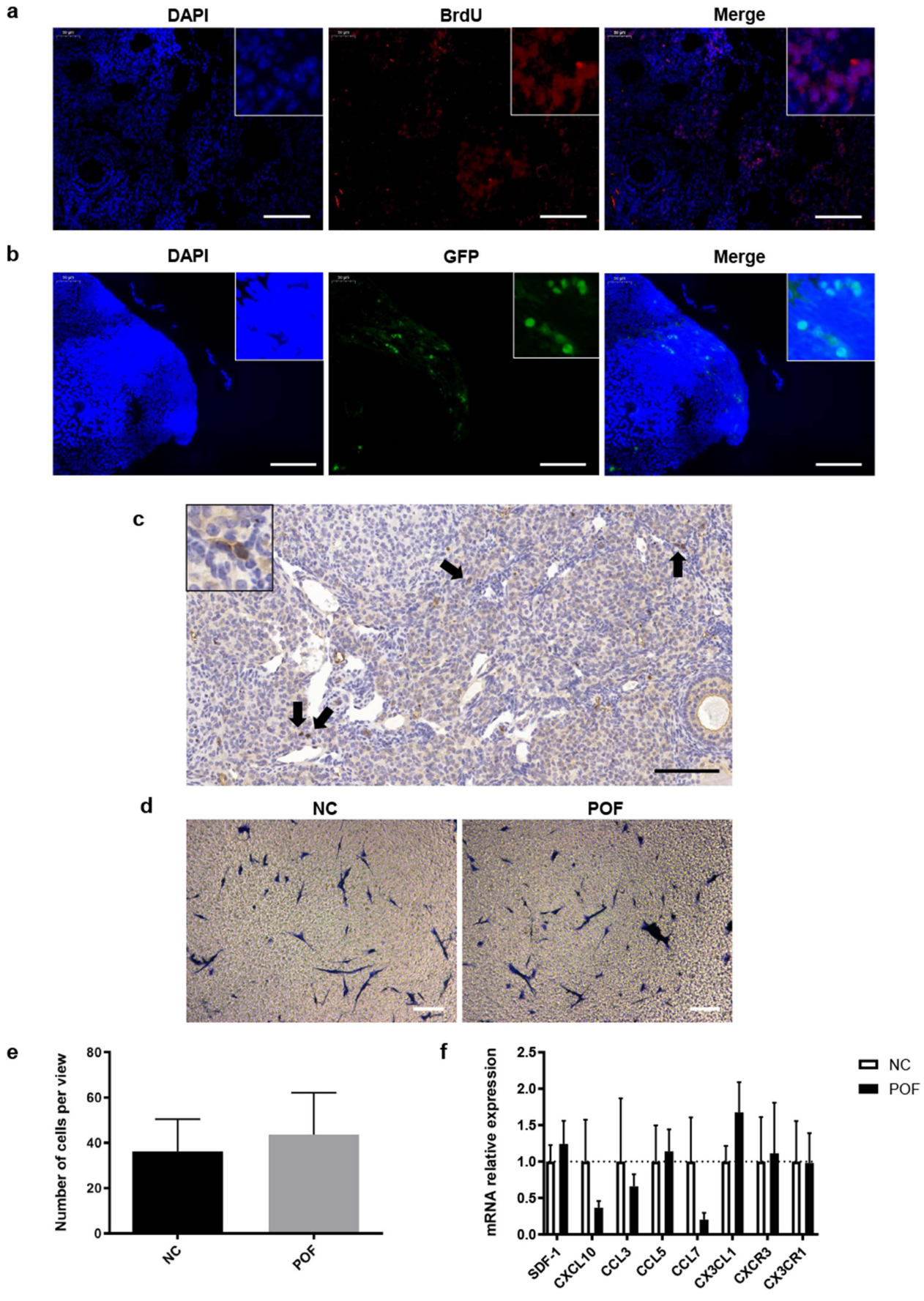
a
DAPI
BrdU
Merge
b
DAPI
GFP
Merge
c
d
NC
POF
e
Number of cells per view
80
60
40
20
0
NC
POF
f
mRNA relative expression
2.5
2.0
1.5
1.0
0.5
0.0
SDF-1
CXCL10
CCL3
CCL5
CCL7
CX3CL1
CXCR3
CX3CR1
NC
POF

◀ **Fig. 5** Location of tail intravenous injected UC-MSCs in the ovaries of POF mice at 2 weeks after treatments. **a** BrdU-labeled, **b** GFP-labeled UC-MSCs, and **c** immunohistochemistry with anti-human nuclei monoclonal antibody were used to track UC-MSCs in vivo. The black arrow represents UC-MSCs. **d** Transwell assays examining the chemotactic capacities of ovarian extracts from normal and POF mice (7 days after the model induction) for UC-MSCs. Scale bar = 100 μm. **e** The mRNA levels of chemotaxis cytokines in ovary tissues from normal and POF mice. **f** After 48-h culturing in the medium containing 10% ovarian extracts from normal and POF mice respectively, the mRNA levels of chemotaxis receptors in UC-MSCs were measured

### UC-MSC-EVs Protected GCs from NM-Induced Injury by Attenuating Cell Apoptosis and Inflammation In Vitro

To further explore whether UC-MSCs protect GCs against chemotherapy via the paracrine pathway, UC-MSC-EVs were used to treat NM-induced injured GCs in vitro. First, UC-MSC-EVs were isolated and characterized. The peak concentration of nanoparticles was at 121.1 nm (98.6%), indicating that the purity of the extracted EVs was good (Fig. 6a). Under TEM, the typical teacup-shaped EVs could be observed (Fig. 6b). Western blot analysis showed that UC-MSC-EVs obtained in this study were positive for Alix and CD9, while negative for Calnexin (Fig. 6c). These results were consistent with the characteristics of EVs. Hence, the extracted UC-MSC-EVs were identified and applied to the following experiments.

After 48-h co-culture, UC-MSC-EVs rescued the survival rate of NM-treated GCs (36.04% ± 12.48% vs. 57.66% ± 11.4%, $P = 0.043$; Fig. 6 d and e). Likewise the results in vivo, UC-MSC-EVs significantly decreased the IL-6 and IL-1β levels in KGN cells compared to those in the NM group (76.71 ± 14.58 pg/mg vs. 109.90 ± 12.24 pg/mg, $P = 0.039$; 17.41 ± 2.76 pg/mg vs. 24.37 ± 3.32 pg/mg, $P = 0.049$; Fig. 6f). The total apoptosis rate in the UC-MSC-EVs group was significantly lower compared to that in the NM group (24.86% ± 2.23% vs. 41.21% ± 6.57%, $P = 0.015$). UC-MSC-EVs predominantly protect GCs against early cell apoptosis induced by NM (19.73% ± 0.79% vs. 36.74% ± 5.53%, $P = 0.006$; Fig. 4 g and h). These results showed that UC-MSC-EVs could protect GCs from chemotherapy by decreasing GC inflammation and apoptotic level in vitro.

## Discussion

UC-MSC transplantation has been shown to restore the damaged ovarian function in the POF models [18, 24, 32–36]. The mechanisms focused on inhibiting GC apoptosis, promoting GC proliferation and ovarian angiogenesis, activating primordial follicles, upregulating the expression of protective growth factors, and the antioxidant effect [33–38]. The activation of the AKT pathway plays a vital role in the reparative effects of UC-MSCs [39, 40]. However, there was no study reporting the inflammation regulatory effects of UC-MSCs on chemotherapy-induced ovarian damage so far, regardless of in vivo or in vitro. The current study attempted to explain the reparative effects of UC-MSCs on POF from both anti-apoptosis and inflammation inhibition. Moreover, we used UC-MSC-EVs to treat chemotherapy-injured GCs to confirm the potential role of a paracrine mechanism. Inhibition of GC apoptosis and inflammation was also ascertained in vitro.

GCs construct the living microenvironment for the oocyte, maintaining oocyte survival and follicle development. Chemotherapeutic agents result in DNA double-strand break, thus inducing the apoptosis of GCs [41, 42]. One of the principal mechanisms to activate cell apoptosis is the mitochondrial pathway, which is regulated by the Bcl-2 family members [43]. In the Bcl-2 family, the pro-apoptotic protein Bax and the anti-apoptotic protein Bcl-xl are common markers for apoptosis, and they have been shown to regulate apoptosis in the ovary [44]. Similar to previous reports [33, 36], we found that UC-MSC treatment reversed the apoptotic level of GCs, as well as inhibited the activation of apoptotic executive enzyme caspase-3 and reduced the Bax/Bcl-xl ratio in the ovaries. These results demonstrated the protective effects of UC-MSCs against the apoptosis in the ovary tissue induced by chemotherapy.

The molecular mechanisms underlying the restorative effect of UC-MSCs remain unclear. AKT and P38 pathways contribute to numerous biological processes, including metabolism, immune regulation, and various aspects of cell development [39]. The phosphorylation of AKT has been evidenced to activate primordial follicle, promote ovarian angiogenesis, increase cell proliferation, and decrease apoptosis in GCs, as well as regulate T cell subset ratios [29, 33, 40]. Here, we also noticed a significantly increased level of phosphorylated AKT after UC-MSC treatment, suggesting that UC-MSCs might recover the damaged ovary via the AKT pathway. However, it needs further study to investigate how UC-MSCs regulate the phosphorylation of AKT in POF. P38 is a member of the mitogen-activated protein kinase (MAPK) family. The regulation of cellular physiology by the MAPK pathway is complex and often controversial. Although the P38 pathway has been shown to play an important role in promoting inflammation and cell apoptosis under stimuli, which was reported in GCs of radiation-induced damaged ovaries [45, 46], other studies showed that the activation of the P38 pathway could produce anti-apoptotic and proliferative effects and promote cell survival in prostate and lung cancers [47]. When responding to chemotherapeutic agents, different organs trigger opposite effects of the P38 pathways, suggesting the dual roles of P38 in genotoxic stress-induced apoptosis [48]. In the current study, P38 phosphorylation was inhibited after chemotherapy, but reversed by UC-MSC transplantation. These

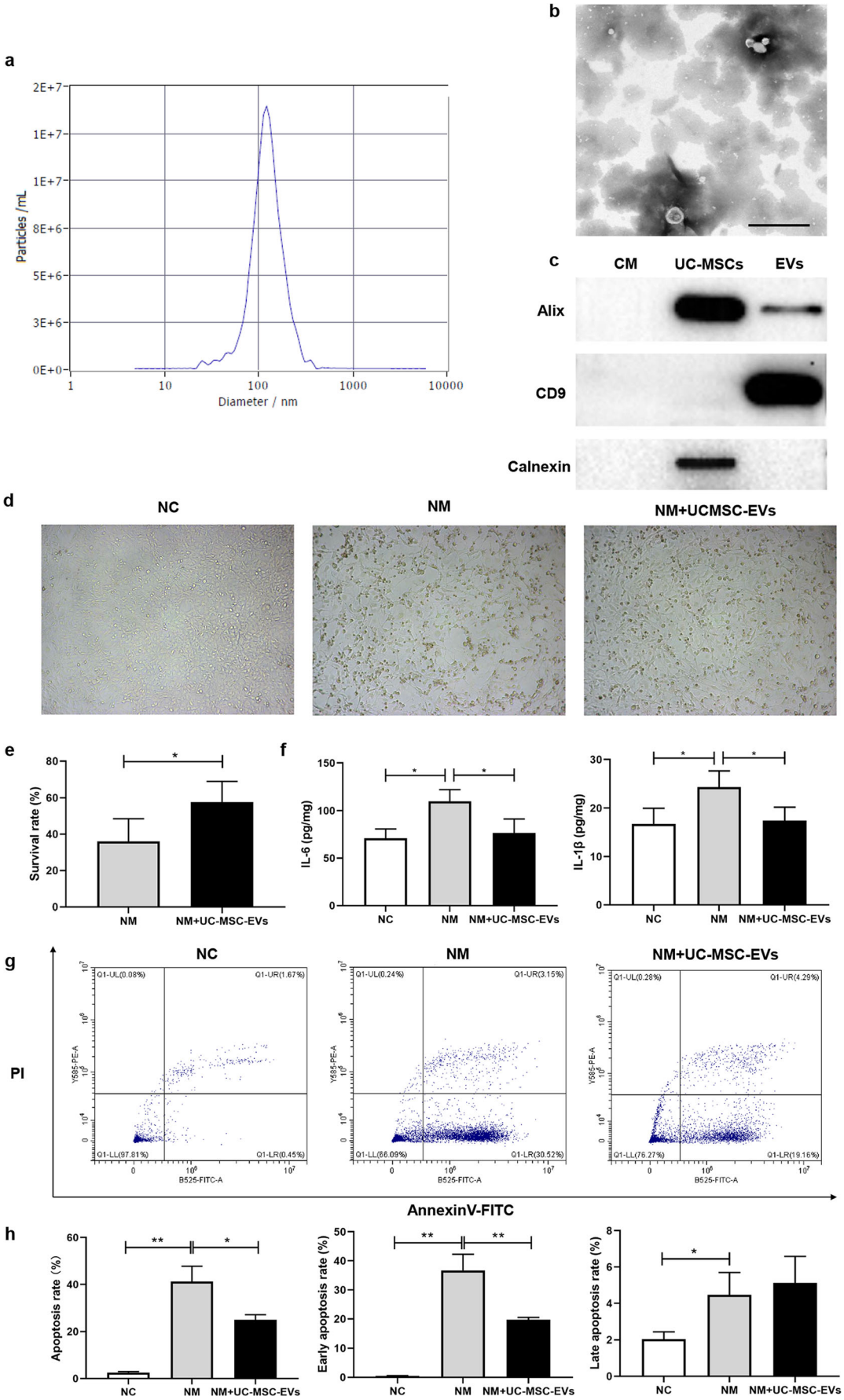
a
Particles /mL
2E+7
1E+7
1E+7
8E+6
5E+6
3E+6
0E+0
1
10
100
1000
10000
Diameter / nm
b
c
CM
UC-MSCs
EVs
Alix
CD9
Calnexin
d
NC
NM
NM+UCMSC-EVs
e
Survival rate (%)
NM
NM+UC-MSC-EVs
f
IL-6 (pg/mg)
IL-1β (pg/mg)
NC
NM
NM+UC-MSC-EVs
g
NC
NM
NM+UC-MSC-EVs
PI
AnnexinV-FITC
Q1-UL(0.08%)
Q1-UR(1.67%)
Q1-LL(97.81%)
Q1-LR(0.45%)
Q1-UL(0.24%)
Q1-UR(3.15%)
Q1-LL(66.09%)
Q1-LR(30.52%)
Q1-UL(0.28%)
Q1-UR(4.29%)
Q1-LL(76.27%)
Q1-LR(19.16%)
h
Apoptosis rate (%)
Early apoptosis rate (%)
Late apoptosis rate (%)
NC
NM
NM+UC-MSC-EVs

◀ **Fig. 6** Identification of UC-MSC-EVs and effects of UC-MSC-EVs on NM-treated granulosa cells in vitro. **a** Nanoparticle tracking analysis, **b** the image under transmission electron microscope, and **c** the protein expression of EV markers for EVs extracted from UC-MSCs culture medium. After NM-KGN cells treated with or without UC-MSC-EVs for 48 h, **d** the morphology of KGN cells was observed, and **e** the survival rates were examined by CCK-8 assays. **f** The IL-6 and IL-1β concentrations of NM-KGN cells (adjusted by the protein concentrations) treated with or without UC-MSC-EVs. **g** Flow cytometric analysis of AnnexinV/PI staining levels of KGN cells. **h** Comparisons of total, early and late apoptosis rates of KGN cells among the three groups. $*P < 0.05$. $**P < 0.01$

results indicated that the pro-survival effect of P38 took predominance in the CTX-induced POF model.

CTX could break the inflammatory balance in the ovaries through inhibiting the production of anti-inflammatory cytokines whereas increasing the production of pro-inflammatory cytokines. Immune regulation and anti-inflammatory property are critical characteristics for MSC treatment, which would help rescue the ovary damage [19, 20, 23]. Skin-derived MSCs and human amnion–derived MSCs could decrease the elevated expression of IL-6, IL-1β, IL-8, and TNF-α in the ovaries damaged by chemotherapy [19, 23]. Bone marrow–derived MSCs (BMSCs) were also reported to help in reversing the increased TNF-α level in chemotherapy-induced POF [22]. Yin et al. used human placenta–derived MSCs to treat autoimmune-induced POF mice and found that the restorative effects were associated with the decreased ratios of Th17/Tc17 and Th17/Treg cells in the spleens [40]. Despite the numerous studies about the immune suppression and anti-inflammatory effects of UC-MSCs in other diseases, they were unrevealed in the POF model. Here, we found decreased expression of IL-6 and IL-1β as well as increased expression of anti-inflammatory cytokines IL-10 and TSG-6 in the UC-MSC group compared to that in the POF group. Despite extensive studies about inflammatory cytokines in the POF model, immune cell infiltrations were rarely examined. Here, the distributions of macrophages and neutrophils were assessed. We found abundant macrophage and neutrophil infiltration in the CTX-damaged ovaries. However, UC-MSC treatment could relieve both macrophage and neutrophil infiltration, leading to the mitigation of ovarian inflammation caused by chemotherapy.

The tracking of UC-MSCs in vivo allowed to preliminarily reveal the mechanism underlying the restorative effects. Most studies have shown that MSCs excrete various cytokines which enhance the proliferation, survival, and function of resident cells to repair tissue damage, thus indicating the significance of a paracrine mechanism [16, 23, 25]. Likewise, UC-MSCs could secrete protective cytokines and growth factors (VEGF, HGF, FGF-2, and IGF-1), and also promoted the ovary tissue to express those cytokines [35]. Additionally, the ability of MSCs to differentiate into GCs in POF mice has been also reported, such as endometrial MSCs [26]. For UC-MSCs, previous studies consistently observed that intravenously injected human stem cells migrated into the ovarian interstitium rather than the follicles [24, 33–35], which is in accordance with our findings. The results implied that the protective effects of UC-MSCs relied on a paracrine mechanism, but not their multipotent differentiation capacity.

EVs as a category of membranous vesicles (including exosomes and microvesicles) secreted by various kinds of cells contain numerous molecules, such as mRNA, microRNAs, lncRNAs, proteins, and lipids [49]. By transferring these contents, EVs mediate communications between cells and modify the biological processes in target cells, participating in the paracrine mechanism. Yang et al. found that UC-MSC-derived microvesicle transplantation recovered ovarian function in POF mice by inducing angiogenesis via the PI3K/AKT pathway [29]. Inhibition of GC stress and apoptosis was also reported to participate in the protective effects of UC-MSC-derived exosomes/EVs against cisplatin-induced ovarian damage [28, 30]. In this study, UC-MSC-EVs could alleviate not only apoptosis level, but also inflammation level of alkylating agent–damaged GCs, thus further ascertaining the vital roles of a paracrine mechanism and the anti-inflammatory effect of UC-MSCs.

Many studies identified the "homing capacity" of MSCs when they found that MSCs in the circulatory system could migrate into the target organs. However, likewise to the first and largest retention of intravenously administered MSCs in the lungs, MSCs could be detained by the capillaries and further infiltrate into the respective organs. Liu et al. examined the homing effects of BMSCs to GCs in vitro with or without cisplatin pretreatment, and GCs injured by cisplatin were found to promote the migration of BMSCs, suggesting the chemoattractiveness of cisplatin-damaged ovaries for BMSCs [50]. In contrast, although Gabr et al. speculated that the elevation of ovarian TNF-α might play a role in the attraction of BMSCs in vivo, they noticed entrapments of BMSCs in the ovarian stroma in both the control and POF groups [22]. Their results were similar to our findings in vitro, and we neither found a difference in the expression of chemokines or relative receptors with or without CTX pretreatment. The chemoattractiveness of injured ovaries for UC-MSCs and underlying mechanisms still need further confirmation and exploration.

Although UC-MSCs were considered as a valuable candidate for treating clinical POF, the treatment protocol, including the administration frequency, is undetermined yet. Restored ovarian functions were usually reported within 6 weeks following the UC-MSC transplantation, [33–35]. In addition, several studies demonstrated a decrease of endometrial MSC count in the ovaries of POF mice over time [16, 26]. Here, we noticed some fluctuations of UC-MSCs reparative

effects after 4 weeks compared to those after 2 weeks. Therefore, a consideration was raised that the retention duration in the ovaries of UC-MSCs in different batches might have some influences on the treatment frequency. Repetitive administrations of UC-MSCs may be necessary for consolidating the effects, and 2 weeks might be a suggested time interval between two treatments for our UC-MSC batch. However, determining the fate and pharmacokinetics of UC-MSCs in vivo still needs further investigation.

## Conclusion

The present study demonstrated that intravenously injected UC-MSCs could rapidly improve the ovarian function in chemotherapy-induced POF through anti-apoptotic and anti-inflammatory effects via the activation of the AKT and P38 pathways. UC-MSCs could migrate to the ovarian stroma and restore the tissues by a paracrine mechanism. Our study provided further evidence for the protective effects of UC-MSC transplantation for chemotherapy-induced POF currently lacking effective treatments. As the paracrine mechanism is one of the predominant methods to achieve the restorative effects of UC-MSCs, UC-MSC-related products, including EVs, might be able to serve as novel therapeutic candidates.

**Abbreviations** UC-MSCs, umbilical cord mesenchymal stem cells; POF, premature ovary failure; HRT, hormone replacement therapy; E2, estradiol; FSH, follicle-stimulating hormone; GC, granulosa cell; CTX, cyclophosphamide; EV, extracellular vesicle; NC, normal control; SD, standard deviation; ANOVA, one-way analysis of variance

**Supplementary Information** The online version contains supplementary material available at https://doi.org/10.1007/s43032-021-00499-1.

**Acknowledgements** The authors would like to thank Wuhan Hamilton Biotechnology-Co. for supplying human UC-MSCs and conditioned culture medium.

**Code Availability** Not applicable.

**Author's Contribution** TR Deng performed in vitro and in vivo experiments and data analysis and wrote the first draft of manuscript; J He and QY Yao performed in vivo experiments; LR Xue and LJ Wu performed in vitro experiments; DC Wu and MF Wu participated in scientific discussion; CY Li and YF Li contributed to the study concept, research design, and data analysis and finalized the manuscript. All the authors have read and approved the final manuscript for submission.

**Funding** This work has been supported by grants from the National Natural Science Foundation of China (81771654), Wuhan Science and Technology Bureau (2019020701011436, 2019030703011513), and the National Key Research and Development Project (2018YFC1002103).

**Data Availability** The data used in the current study are available from the corresponding author on a reasonable request.

## Declarations

**Ethics Approval and Consent to Participate** All animal experiments were approved by the Institutional Review Board of Tongji Hospital, Tongji Medical College, Huazhong University of Science and Technology (ID: TJ-A20180701).

**Consent for Publication** This manuscript describes original work and is not under consideration by any other journal. All authors have read the manuscript and approved this version for submission.

**Conflict of Interest** The authors declare no competing interests.

## References

1. European Society for Human Reproduction, Embryology Guideline Group on P. O. I., Webber L., Davies M., Anderson R., Bartlett J., et al. ESHRE Guideline: management of women with premature ovarian insufficiency. Hum Reprod. 2016;31(5):926–37.
2. Morgan S, Anderson RA, Gourley C, Wallace WH, Spears N. How do chemotherapeutic agents damage the ovary? Hum Reprod Update. 2012;18(5):525–35.
3. Bines J, Oleske DM, Cobleigh MA. Ovarian function in premenopausal women treated with adjuvant chemotherapy for breast cancer. J Clin Oncol. 1996;14(5):1718–29.
4. Lower EE, Blau R, Gazder P, Tummala R. The risk of premature menopause induced by chemotherapy for early breast cancer. J Womens Health Gend Based Med. 1999;8(7):949–54.
5. Meirow D. Reproduction post-chemotherapy in young cancer patients. Mol Cell Endocrinol. 2000;169(1-2):123–31.
6. Webber L, Anderson RA, Davies M, Janse F, Vermeulen N. HRT for women with premature ovarian insufficiency: a comprehensive review. Hum Reprod Open. 2017;2017(2):hox007.
7. Bochon B, Kozubska M, Surygala G, Witkowska A, Kuzniewicz R, Grzeszczak W, et al. Mesenchymal stem cells-potential applications in kidney diseases. Int J Mol Sci. 2019;20:10.
8. Behnke J, Kremer S, Shahzad T, Chao CM, Bottcher-Friebertshauser E, Morty RE, et al. MSC based therapies-new perspectives for the injured lung. J Clin Med. 2020;9:3.
9. Doyle EC, Wragg NM, Wilson SL. Intraarticular injection of bone marrow-derived mesenchymal stem cells enhances regeneration in knee osteoarthritis. Knee Surg Sports Traumatol Arthrosc. 2020;28:3827–42.
10. Liu X, Xu W, Zhang Z, Liu H, Lv L, Han D, et al. Vascular endothelial growth factor-transfected bone marrow mesenchymal stem cells improve the recovery of motor and sensory functions of rats with spinal cord injury. Spine (Phila Pa 1976). 2020;45(7):E364–E72.
11. Cao Y, Sun H, Zhu H, Zhu X, Tang X, Yan G, et al. Allogeneic cell therapy using umbilical cord MSCs on collagen scaffolds for patients with recurrent uterine adhesion: a phase I clinical trial. Stem Cell Res Ther. 2018;9(1):192.
12. Sheikhansari G, Aghebati-Maleki L, Nouri M, Jadidi-Niaragh F, Yousefi M. Current approaches for the treatment of premature ovarian failure with stem cell therapy. Biomed Pharmacother. 2018;102:254–62.
13. Bongso A, Fong CY. The therapeutic potential, challenges and future clinical directions of stem cells from the Wharton's jelly of the human umbilical cord. Stem Cell Rev. 2013;9(2):226–40.
14. Blumenfeld Z. Gynaecologic concerns for young women exposed to gonadotoxic chemotherapy. Curr Opin Obstet Gynecol. 2003;15(5):359–70.

15. Mohamed SA, Shalaby SM, Abdelaziz M, Brakta S, Hill WD, Ismail N, et al. Human mesenchymal stem cells partially reverse infertility in chemotherapy-induced ovarian failure. Reprod Sci. 2018;25(1):51–63.
16. Wang Z, Wang Y, Yang T, Li J, Yang X. Study of the reparative effects of menstrual-derived stem cells on premature ovarian failure in mice. Stem Cell Res Ther. 2017;8(1):11.
17. Su J, Ding L, Cheng J, Yang J, Li X, Yan G, et al. Transplantation of adipose-derived stem cells combined with collagen scaffolds restores ovarian function in a rat model of premature ovarian insufficiency. Hum Reprod. 2016;31(5):1075–86.
18. Zheng Q, Fu X, Jiang J, Zhang N, Zou L, Wang W, et al. Umbilical cord mesenchymal stem cell transplantation prevents chemotherapy-induced ovarian failure via the NGF/TrkA pathway in rats. Biomed Res Int. 2019;2019:6539294.
19. Lai D, Wang F, Dong Z, Zhang Q. Skin-derived mesenchymal stem cells help restore function to ovaries in a premature ovarian failure mouse model. PLoS One. 2014;9(5):e98749.
20. Luo Q, Yin N, Zhang L, Yuan W, Zhao W, Luan X, et al. Role of SDF-1/CXCR4 and cytokines in the development of ovary injury in chemotherapy drug induced premature ovarian failure mice. Life Sci. 2017;179:103–9.
21. Fathollahi A, Gabalou NB, Aslani S. Mesenchymal stem cell transplantation in systemic lupus erythematous, a mesenchymal stem cell disorder. Lupus. 2018;27(7):1053–64.
22. Gabr H, Rateb MA, El Sissy MH, Ahmed SH. Ali Abdelhameed Gouda S. The effect of bone marrow-derived mesenchymal stem cells on chemotherapy induced ovarian failure in albino rats. Microsc Res Tech. 2016;79(10):938–47.
23. Ling L, Feng X, Wei T, Wang Y, Wang Y, Zhang W, et al. Effects of low-intensity pulsed ultrasound (LIPUS)-pretreated human amnion-derived mesenchymal stem cell (hAD-MSC) transplantation on primary ovarian insufficiency in rats. Stem Cell Res Ther. 2017;8(1):283.
24. Zhu SF, Hu HB, Xu HY, Fu XF, Peng DX, Su WY, et al. Human umbilical cord mesenchymal stem cell transplantation restores damaged ovaries. J Cell Mol Med. 2015;19(9):2108–17.
25. Ling L, Feng X, Wei T, Wang Y, Wang Y, Wang Z, et al. Human amnion-derived mesenchymal stem cell (hAD-MSC) transplantation improves ovarian function in rats with premature ovarian insufficiency (POI) at least partly through a paracrine mechanism. Stem Cell Res Ther. 2019;10(1):46.
26. Lai D, Wang F, Yao X, Zhang Q, Wu X, Xiang C. Human endometrial mesenchymal stem cells restore ovarian function through improving the renewal of germline stem cells in a mouse model of premature ovarian failure. J Transl Med. 2015;13:155.
27. Hong L, Yan L, Xin Z, Hao J, Liu W, Wang S, et al. Protective effects of human umbilical cord mesenchymal stem cell-derived conditioned medium on ovarian damage. J Mol Cell Biol. 2020;12(5):372–85.
28. Zhang J, Yin H, Jiang H, Du X, Yang Z. The protective effects of human umbilical cord mesenchymal stem cell-derived extracellular vesicles on cisplatin-damaged granulosa cells. Taiwan J Obstet Gynecol. 2020;59(4):527–33.
29. Yang Z, Du X, Wang C, Zhang J, Liu C, Li Y, et al. Therapeutic effects of human umbilical cord mesenchymal stem cell-derived microvesicles on premature ovarian insufficiency in mice. Stem Cell Res Ther. 2019;10(1):250.
30. Sun L, Li D, Song K, Wei J, Yao S, Li Z, et al. Exosomes derived from human umbilical cord mesenchymal stem cells protect against cisplatin-induced ovarian granulosa cell stress and apoptosis in vitro. Sci Rep. 2017;7(1):2552.
31. Yin L, Liu X, Shi Y, Ocansey DKW, Hu Y, Li X, et al. Therapeutic advances of stem cell-derived extracellular vesicles in regenerative medicine. Cells. 2020;9:3.
32. Shen J, Cao D, Sun JL. Ability of human umbilical cord mesenchymal stem cells to repair chemotherapy-induced premature ovarian failure. World J Stem Cells. 2020;12(4):277–87.
33. Zhang J, Xiong J, Fang L, Lu Z, Wu M, Shi L, et al. The protective effects of human umbilical cord mesenchymal stem cells on damaged ovarian function: a comparative study. Biosci Trends. 2016;10(4):265–76.
34. Song D, Zhong Y, Qian C, Zou Q, Ou J, Shi Y, et al. Human umbilical cord mesenchymal stem cells therapy in cyclophosphamide-induced premature ovarian failure rat model. Biomed Res Int. 2016;2016:2517514.
35. Li J, Mao Q, He J, She H, Zhang Z, Yin C. Human umbilical cord mesenchymal stem cells improve the reserve function of perimenopausal ovary via a paracrine mechanism. Stem Cell Res Ther. 2017;8(1):55.
36. Yang Y, Lei L, Wang S, Sheng X, Yan G, Xu L, et al. Transplantation of umbilical cord-derived mesenchymal stem cells on a collagen scaffold improves ovarian function in a premature ovarian failure model of mice. In Vitro Cell Dev Biol Anim. 2019;55(4):302–11.
37. Ding L, Yan G, Wang B, Xu L, Gu Y, Ru T, et al. Transplantation of UC-MSCs on collagen scaffold activates follicles in dormant ovaries of POF patients with long history of infertility. Sci China Life Sci. 2018;61(12):1554–65.
38. Wang S, Yu L, Sun M, Mu S, Wang C, Wang D, et al. The therapeutic potential of umbilical cord mesenchymal stem cells in mice premature ovarian failure. Biomed Res Int. 2013;2013:690491.
39. Liu M, Qiu Y, Xue Z, Wu R, Li J, Niu X, et al. Small extracellular vesicles derived from embryonic stem cells restore ovarian function of premature ovarian failure through PI3K/AKT signaling pathway. Stem Cell Res Ther. 2020;11(1):3.
40. Yin N, Wang Y, Lu X, Liu R, Zhang L, Zhao W, et al. hPMSC transplantation restoring ovarian function in premature ovarian failure mice is associated with change of Th17/Tc17 and Th17/Treg cell ratios through the PI3K/Akt signal pathway. Stem Cell Res Ther. 2018;9(1):37.
41. Bedoschi GM, Navarro PA, Oktay KH. Novel insights into the pathophysiology of chemotherapy-induced damage to the ovary. Panminerva Med. 2019;61(1):68–75.
42. Bedoschi G, Navarro PA, Oktay K. Chemotherapy-induced damage to ovary: mechanisms and clinical impact. Future Oncol. 2016;12(20):2333–44.
43. Hussein MR, Haemel AK, Wood GS. Apoptosis and melanoma: molecular mechanisms. J Pathol. 2003;199(3):275–88.
44. Cory S, Adams JM. The Bcl2 family: regulators of the cellular life-or-death switch. Nat Rev Cancer. 2002;2(9):647–56.
45. Uma J, Muraly P, Verma-Kumar S, Medhamurthy R. Determination of onset of apoptosis in granulosa cells of the preovulatory follicles in the bonnet monkey (Macaca radiata): correlation with mitogen-activated protein kinase activities. Biol Reprod. 2003;69(4):1379–87.
46. Mantawy EM, Said RS, Abdel-Aziz AK. Mechanistic approach of the inhibitory effect of chrysin on inflammatory and apoptotic events implicated in radiation-induced premature ovarian failure: emphasis on TGF-beta/MAPKs signaling pathway. Biomed Pharmacother. 2019;109:293–303.
47. Koul HK, Pal M, Koul S. Role of p38 MAP kinase signal transduction in solid tumors. Genes Cancer. 2013;4(9-10):342–59.
48. Sui X, Kong N, Ye L, Han W, Zhou J, Zhang Q, et al. p38 and JNK MAPK pathways control the balance of apoptosis and autophagy in

response to chemotherapeutic agents. Cancer Lett. 2014;344(2): 174–9.

49. Wahlgren J, Statello L, Skogberg G, Telemo E, Valadi H. Delivery of small interfering RNAs to cells via exosomes. Methods Mol Biol. 2016;1364:105–25.

50. Liu J, Zhang H, Zhang Y, Li N, Wen Y, Cao F, et al. Homing and restorative effects of bone marrow-derived mesenchymal stem cells on cisplatin injured ovaries in rats. Mol Cell. 2014;37(12):865–72.